Pablo Giunta
Máximo Moreno
Fernando Mariño
Norma Amadeo
Miguel Laborde

Laboratorio de Procesos Catalíticos, Facultad de Ingeniería, Universidad de Buenos Aires, Buenos Aires, Argentina.

Research Article

COPROX Fixed Bed Reactor – Temperature Control Schemes

Different temperature control schemes for the COPROX stage of a 5-kW fuel cell system were analyzed. It was found that, among the schemes proposed, i.e., co- and countercurrent heat exchange, single adiabatic reactor and series of adiabatic reactors with interstage heat exchange, the best choice for temperature control was the series of adiabatic reactors with interstage heat exchange. This scheme represented the best way to keep the average temperature around 443 K, which was found to be the most suitable temperature for selectivity towards CO oxidation. If hydrogen is produced from ethanol steam reforming, the heat withdrawal can be carried out by the water/ethanol reformer feed mixture, thus contributing to the energy integration of the overall system.

Keywords: Chemical reactors, CO preferential oxidation, Heat transfer, Reactor design, Reactor modeling

Received: November 30, 2011; *revised:* January 9, 2012; *accepted:* February 6, 2012

DOI: 10.1002/ceat.201100644

1 Introduction

Among the different types of fuel cells, the PEMFC is the most adequate for mobile applications because of its high power density, low weight and relatively low operating temperature. A disadvantage of this fuel cell type is its high sensitivity to the presence of CO in the feed gas; a CO concentration of 50 ppm is enough to quickly poison the anode. When H_2 is produced from reforming or partial oxidation of alcohols or hydrocarbons, the formation of carbon oxides (CO_2 and CO, the latter in the range of 8–12 %) is inevitable. To reduce the CO concentration in the feed, a water-gas shift (WGS) reactor is used. Nevertheless, the WGS product gas contains about 1 % CO because of thermodynamic limitations [1]. Different techniques for the last purification are proposed, for example, pressure swing absorption, H_2 separation by Pd membranes, CO methanation and CO preferential oxidation (COPrOx). The last one is a good alternative because of its simplicity and cost effectiveness. An air stream is added to the feed gas and, in the presence of a suitable catalyst, CO is oxidized to CO_2. Since there is a high amount of H_2 in the stream, the oxidation must be very selective towards CO. Noble metals, particularly Pt [2, 3], Au [4] and Ru [5], and some nonprecious metals such as Co, Cr, Cu, Ni and Zn supported on ceria-zirconia [6] were used as catalysts. Nevertheless, it was also demonstrated that other catalysts such as Cu-Ce, less expensive than Pt, are very active and selective [7–9]. In the COPrOx reactor the following reactions occur in the gas phase[1)]:

$$CO + \frac{1}{2}O_2 \rightarrow CO_2 \quad \Delta H_{r_1} = -283\,\mathrm{kJ\,mol^{-1}} \tag{1}$$

$$H_2 + \frac{1}{2}O_2 \rightarrow H_2O \quad \Delta H_{r_2} = -242\,\mathrm{kJ\,mol^{-1}} \tag{2}$$

Few papers were published concerning the design and optimization of the COPROX reactor. Most of them assumed a fixed bed reactor and noble metal based catalysts. Zalc and Löffler [10] pointed out that reactor temperature control is crucial due to the reaction kinetics and the narrow temperature operation range to achieve high selectivity for the desired reaction (1). Oliva et al. [11] analyzed the COPrOx reactor design as a component of the CO clean-up system of the ethanol processor for H_2 production applied to PEM fuel cells. An eggshell catalyst type of Pt/Al_2O_3 was considered by the authors. They found that the results strongly depend on the

Correspondence: Dr. F. Mariño (fernando@di.fcen.uba.ar), Laboratorio de Procesos Catalíticos, Facultad de Ingeniería, Universidad de Buenos Aires, Pabellón de Industrias, Ciudad Universitaria, 1428 Buenos Aires, Argentina.

1) List of symbols at the end of the paper.

particular catalyst and on the considered inlet/outlet specifications. Lee et al. [12] developed a preferential oxidation (PrOx) reactor for a 10-kWe PEMFC by using a Pt-Ru/Al_2O_3 based catalyst. The authors proposed two-stage in-series multitubular adiabatic reactors with interstage cooling. In this way, the pressure drop is diminished and the hot spots in the bed are avoided. Dudfield et al. [13, 14] also used a Pt/Ru based catalyst supported on the surface of a finned-type heat exchanger. The authors designed a compact unit of a PrOx reactor treating a gaseous stream in a methanol processor for PEMFC for mobile applications; they reduced the initial CO concentration from 0.5 % to less than 20 ppm. Cipití and Recupero [15] developed a 2D steady-state reactor model, driving the design of a single-stage multitube reactor to overcome the system issues of heat management, considering Pt/Al_2O_3 catalysts (pellets of 3 mm × 3 mm) and a cocurrent air in the cooling jacket. Simulation results indicated that the reactor performance strongly depends on the O_2/CO molar ratio, GHSV and inlet temperature. In a previous paper [16], the same research group showed that an optimal temperature control can be achieved by using a configuration with a cocurrent air flow. More recently, nonconventional reactors were used in the COPrOx reaction. Zhou et al. [17] developed a monolithic PrOx reactor for a 5 kW methanol reformer system obtaining concentration levels of CO lower than 50 ppm. Lopez et al. [4], using a Au based catalyst, designed, manufactured and tested a folded-plate reactor for the selective CO oxidation in a H_2-rich feed. A compact reactor with distributed air-side feeds meets the requirements of reducing the CO content in the reforming from 1 % to around 50 ppm for a total flow corresponding to a load of 1.5 kW. Other authors [18–20] also worked on microreactors applied to COPrOx reaction. Finally, O'Connell et al. [21] designed and evaluated one-stage WGS and PrOx reactors for the clean-up of surrogate diesel reformate by using catalysts provided by Johnson Matthey. The authors claim that the PrOx reactor was capable of converting a feed concentration of 1.0 mol.-% CO to 20 ppm.

The particular feature of the system is the temperature increase due to the high exothermicity of both reactions. The aim of this work was to analyze different schemes of heat transfer in a fixed bed reactor for a 5 kW PEM fuel cell using CuO-CeO_2 based catalysts, which make the system selective towards CO oxidation: a) heat exchange, b) adiabatic regime. For case a) a shell and tube equipment in which the reaction occurs inside the tube and the heat exchanging fluid flows through the shell was considered. The reaction was supposed to occur inside the tubes to guarantee better heat exchange. The catalytic material was considered to have a low characteristic length, which enhances the contact with the catalyst.

2 Methodology

To design the fixed bed reactor, a plug flow model was assumed. Heat and mass transfer resistances, both in the film and into the catalyst, were discarded [22]. Heat capacity of species and enthalpy of the reactions were considered constants since no substantial change in these values was observed.

Mass and energy balances for the reaction fluid (RF) in each tube of the multitubular reactor system are:

$$\frac{dF_j}{dz} = \sum_{i=1}^{NR} a_{ij}(\eta_i r_i) A_{cs} \tag{3}$$

$$\frac{dT}{dz} = \frac{\sum_{i=1}^{NR} \left(-\Delta H_{r_i}\right)(\eta_i r_i) A_{cs} + \frac{4}{d_i} U(T^c - T)}{\sum_{j=1}^{NC} F_j Cp_j} \tag{4}$$

$$\frac{dP}{dz} = -g_c \left[150(1-\varepsilon_B)^2 \frac{\mu}{d_p G} + 1.75\right] \frac{G^2}{A_{cs} d_p \rho} \frac{1-\varepsilon_B}{\varepsilon_B^3} \tag{5}$$

The reaction kinetic expressions are given by Lee et al. [8]:

$$-r_{CO} = k_{CO} p_{CO}^{0.91} p_{CO_2}^{-0.37} p_{H_2}^{-0.62} \tag{6}$$

$$-r_{H_2} = k_{H_2} p_{H_2} p_{H_2O}^{-0.69} p_{CO_2}^{-0.48} \tag{7}$$

$$k_{CO}^0 = 3.410^7 \text{mol g}^{-1}\text{s}^{-1}\text{atm}^{0.08} \quad E_{CO} = 94.4 \text{ kJ mol}^{-1}$$
$$k_{H_2}^0 = 6.110^{10} \text{mol g}^{-1}\text{s}^{-1}\text{atm}^{0.17} \quad E_{H_2} = 142 \text{ kJ mol}^{-1}$$

It should be noted that $E_{H2} > E_{CO}$ and that high temperatures favor the reaction with higher activation energy.

There are few publications related to kinetic studies of the COPrOx reaction using Cu-Ce catalysts and assuming the power law as a model. Moreno et al. [9], working with a copper catalyst impregnated on cerium oxide, suggested a power law kinetics for the CO oxidation reaction where the reaction order of CO varied between 0.67 and 0.77 and the reaction order of O_2 was practically zero. Schönbrod et al. [23], using a mixture of copper and cerium oxides as catalysts, postulated power-law type kinetics for the CO oxidation reaction, in which the reaction order of CO was less than 1 and the reaction order of O_2 was practically zero. This work also showed that the partial pressure of H_2 did not significantly affect the reaction rate of CO, which is in agreement with the results obtained by Lee and Kim [8]. Both works [8, 23] concluded that the presence of H_2O and CO_2 in the feed decreased catalyst activity. Other authors [7, 24, 25] proposed a Mars van Krevelen type kinetics for CO oxidation over Cu-Ce catalysts. In summary, only Lee and Kim [8] investigated the kinetics of CO oxidation and H_2 oxidation simultaneously over CuO-CeO_2 catalysts, and they proposed power law type kinetic expressions for both oxidation reactions.

Selectivity is defined as:

$$S = \frac{F_{CO}^e x_{CO}}{F_{H_2}^e x_{H_2}} \tag{8}$$

The heat exchanging fluid (HEF) employed was the ethanol-water mixture to feed the steam reformer, liquid at room temperature [26–28]. Mass and momentum balances were not considered. Co- and countercurrent flow systems were evaluated.

The energy balance is:

$$\frac{dT^c}{dz} = \pm n_t \frac{4}{d_i} \frac{U(T^c - T)}{\sum_{j=1}^{NC} F_j^c Cp_j^c} \quad (9)$$

where n_t is the number of tubular reactors, and superscript 'c' stands for "heat exchanging fluid". HEF exchanges heat with all of the tubes, whereas the presence of multiple tubes in Eq. (4) is not explicit but has its influence through T^c. '+' is applicable to the countercurrent scheme, whereas '–' is employed for the cocurrent scheme. As in the case of the reactor, heat capacities were held constant for the same reasons previously stated. The large exothermicity of both reactions makes the differential equations to be stiff. To improve the convergence, the implicit Euler method was employed [29].

3 Results and Discussion

Simulations for a 5-kW PEM fuel cell were performed for a fixed catalyst load and reactor volume in order to focus the analysis on the heat transfer schemes. The basic conditions are listed in Tab. 1. The catalyst characteristic length was assumed small enough to consider the reaction to be in chemical control ($\eta_i = 1$). An immediate consequence of this was a low catalyst load per unit volume. The main drawback for a low catalyst density was the large volume required for the reaction. This work considered an eggshell-type catalyst pellet.

Since the catalyst bed density was assumed to be constant, the reaction length L, which corresponds to the total catalytic bed (or sum of catalytic beds in the case of a series of reactors), was also fixed.

Table 1. Simulation conditions (per tube) used in this work for a 5 kW PEM fuel cell requirement.

F_T	0.12	mol s^{-1}
F^c_T	0.0732	mol s^{-1}
y_{CO}	0.01	–
y_{CO_2}	0.18	–
y_{O_2}	0.01	–
y_{H_2}	0.5	–
y_W	0.3	–
y_{N_2}	0.01	–
$T^{c,e}$	298	K
P	3	atm
d_i	1.804	cm
n_t	10	–
ρ_B	0.1	g cm^{-3}
L	250	cm

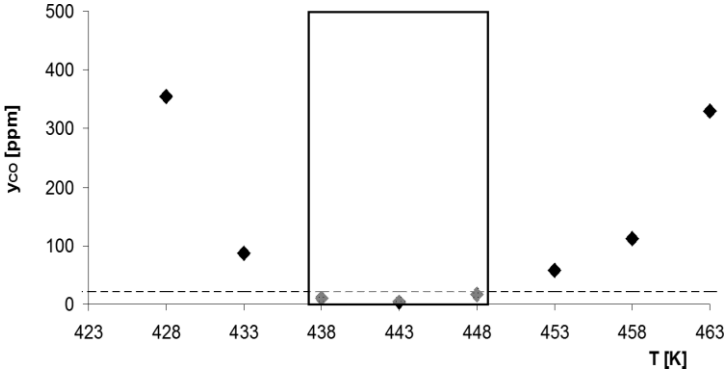

Figure 1. CO exit molar fraction vs. reactor temperature.

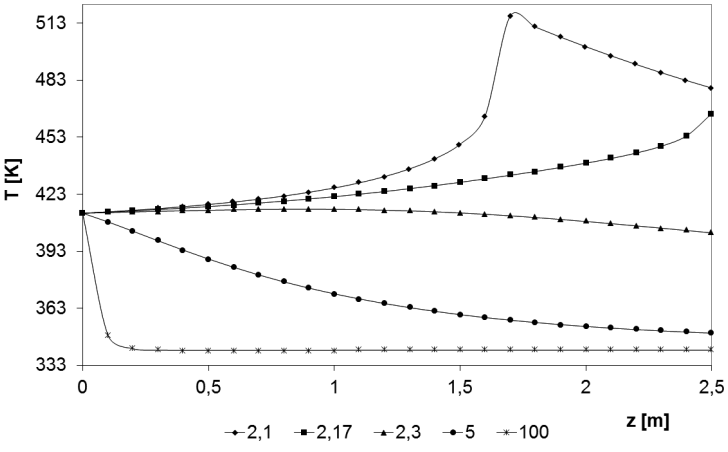

Figure 2. RF temperature profiles for different U and cocurrent heat exchange.

3.1 Heat Exchange Schemes

To identify the range in which the RF temperature should be to fulfill the requirements of the CO fraction, an isothermal reactor was simulated. Results are shown in Fig. 1. From this data it was possible to infer that any scheme should maintain the reactor temperature around 443 K for the fixed catalyst load employed. The following alternatives were analyzed.

3.1.1 Cocurrent Heat Exchange

In this scheme, as the HEF was always colder than the RF, the former always withdrew heat from the latter. Thus, a temperature rise was expected in the HEF, whereas the RF could either decrease or increase its temperature depending on the relative values of the heat generated by reaction and the heat withdrawn (see Eq. (4)), as depicted in Fig. 2. This analysis suggested that, in this scheme, the temperature of the RF could either show a hot spot or decrease until reactions ceased.

When U decreased, temperature rose and so did both conversions (see Figs. 3a and 3b). The activation energy of the H_2 oxidation is higher than that of the CO oxidation; therefore, as the values of U decrease, temperature rise becomes greater, favoring H_2 oxidation and producing a drop in selectivity (see Fig. 3c). Thus, for poor heat transfers, the O_2 was consumed preferably by the H_2 oxidation and the CO conversion was not complete. The abrupt slope change in Figs. 2 and 3 was due to the O_2 complete depletion (it must be noticed that neither r_{CO} nor r_{H2} depend on O_2).

On the other hand, lowering the temperature to favor the selectivity towards CO oxidation had the penalty of decreasing its rate of reaction, which forced to design a larger reactor. Analyzing Fig. 3, it can be said that there was a trade-off in the value of U: if it was too high, the CO oxidation would not proceed, and if it was too low, there would be a loss in selectivity. Fig. 3 shows a high sensitivity in U when complete CO oxidation is expected.

With $T^e = 413$ K, the lower CO fraction was ca. 113.6 ppm, which was too high for the service required. However, better performance was achieved when raising the inlet temperature and U as well. In this way, the thermal level was high enough to reach a CO fraction lower than 20 ppm in the reactor (which had a fixed catalyst load), with the penalty of loss in selectivity. Fig. 4 shows the results for a higher value of T^e.

3.1.2 Countercurrent Heat Exchange

In the countercurrent scheme, the thermal contact of fluid elements of both sides of the heat exchanging boundary introduces an energy feedback effect. The following analysis only covered the effect of U. The analysis of other parameters like T^e will be analyzed in a future work.

The performance of this scheme for different values of U and T^e is presented in Fig. 5. As can be seen, for certain values of U there is a region of inlet temperatures in which multiplicity of steady states was obtained. The sources of this phenomenon were the energy feedback introduced by the contact of the fluids and the nonmonotonic behavior of the kinetics along the reactor (temperature rises when CO and H_2 are oxidized and this tends to increase both reaction rates, while the depletion of CO and H_2 tends to decrease the corresponding rates).

It must, however, be highlighted that, when the RF temperature descends below ca. 370 K, condensation should be expected since the partial pressure of water is essentially constant at a value of roughly 0.9 atm. This condition is not desirable and, besides, the model does not account for phase change. Thus, results corresponding to temperatures below 370 K (below the horizontal dashed line in Fig. 5) were discarded.

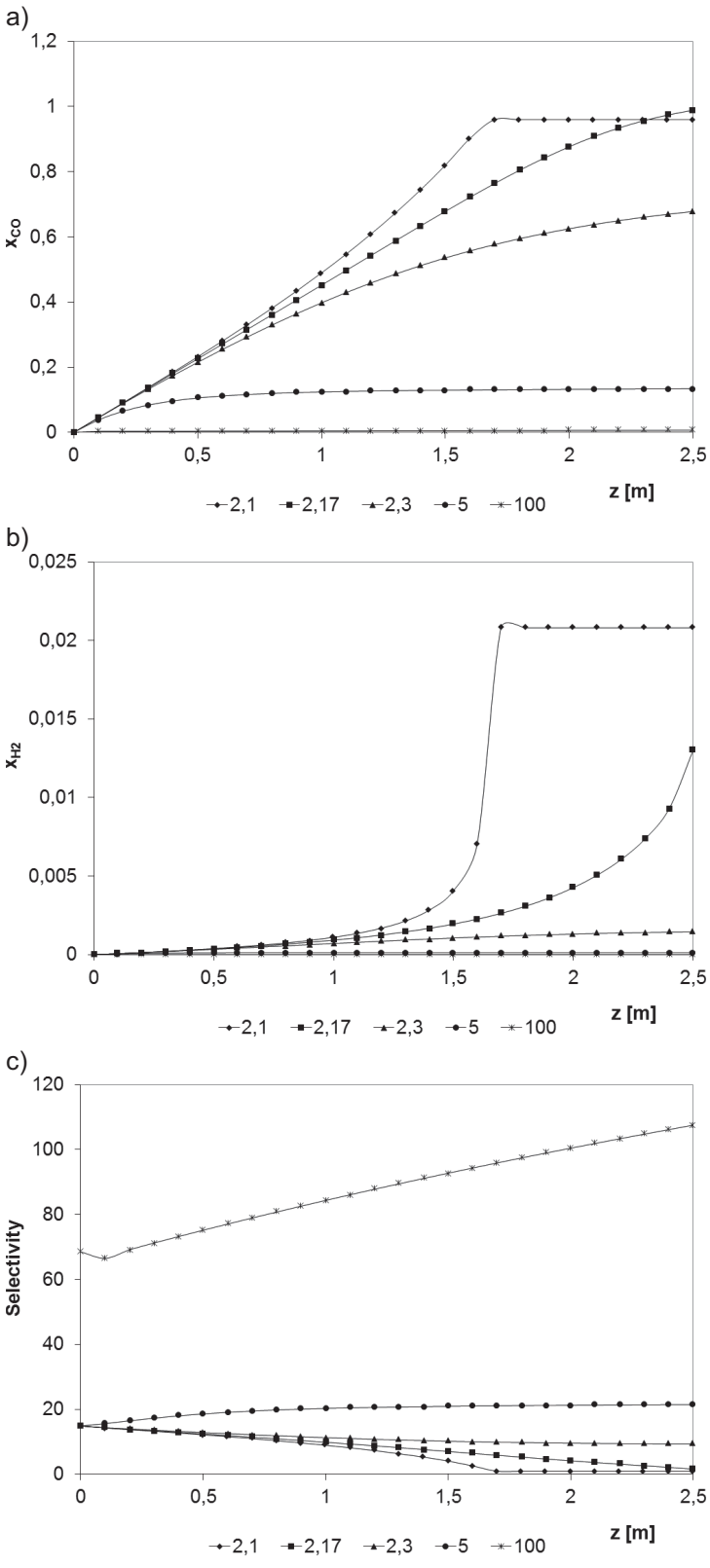

Figure 3. Profiles of a) CO conversion, b) H_2 conversion, and c) selectivity for different values of U at T^e = 413 K and cocurrent heat exchange.

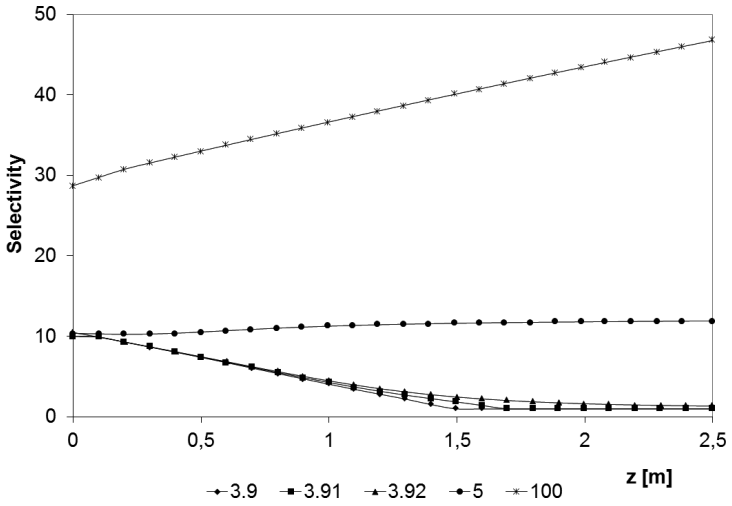

Figure 4. Selectivity profiles for different values of U at T^e = 423 K and cocurrent heat exchange.

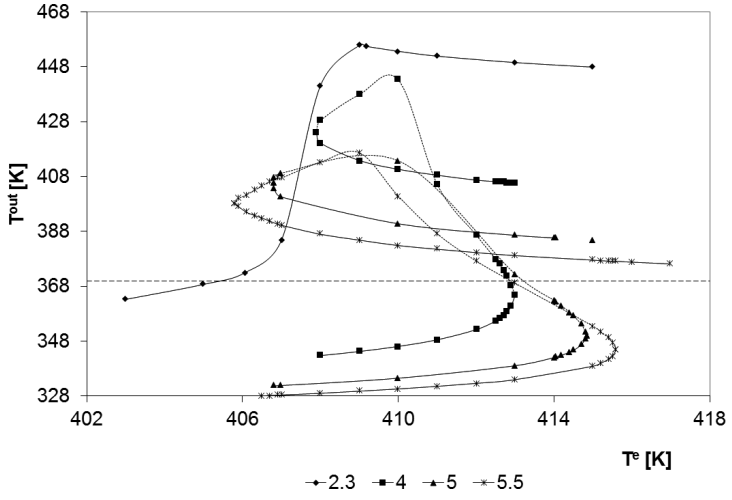

Figure 5. RF outlet temperature vs. RF inlet temperature for different U and countercurrent heat exchange.

When multiplicity is verified, the curves have three branches corresponding to the higher, middle and lower steady states. Fig. 5 also shows that multiplicity is not expected for values of U lower than ca. 3 $W m^{-2}K^{-1}$. Fig. 6 shows the outlet CO molar fraction for the same values of U.

It can be seen that only the middle steady states were capable of meeting the requirements of the PEM fuel cell. Nevertheless, this condition was unstable and, without automatic control, the system would be expected to converge to either the higher or the lower steady state, none of which had a desirable CO depletion; the higher steady state operated at too high temperatures and the H_2 oxidation was favored; the lower steady states operated at too low temperatures, and both rates were slow (and besides, water condensates).

3.2 Adiabatic Regime

3.2.1 Single Adiabatic Fixed Bed Reactor

In this scheme, the only variable to handle was the inlet temperature. As expected, temperature increased throughout the reactor until complete depletion of O_2 (see Fig. 7a). Accordingly, since $E_{CO} < E_{H2}$, selectivity towards CO decreased (see Fig. 7b).

Fig. 8 shows the strong sensitivity of the reactor performance with respect to T^e in the range of 383–388 K. Within this range, when T^e increased, the system was kinetically favored and the outlet CO fraction decreased. On the other hand, the average temperature was low enough so as to maintain relatively high selectivity.

For T^e > 388 K, y_{CO} increased with increasing T^e due to the drop in selectivity caused, in turn, by the higher average temperature. In the whole temperature range analyzed, the lowest CO fraction obtained was ca.1400 ppm, far beyond the 20 ppm required.

3.2.2 Series of Adiabatic Fixed Bed Reactors and Heat Exchanges

The main drawback in the single adiabatic reactor shema was the runaway behavior of the reactor, which caused the consumption of O_2 mainly through H_2 oxidation. To overcome this problem, a series of adiabatic reactors with interstage cooling was employed in order to improve temperature control. In this scheme, the RF enters an adiabatic reactor in which temperature increases, passes through a heat exchanger where the RF is cooled using the HEF defined in Sect. 2 as the cold stream, and finally enters the next adiabatic reactor.

The key variables for temperature control were the reactor lengths and the RF feed temperatures of each reactor. The temperature range should be high enough for the CO oxidation reaction to proceed and low enough so as not to lose selectivity. Figs. 9 and 10 show the evolution of temperature, selectivity and CO and O_2 mole fractions throughout the reactor for two feed temperatures. Also, reactor lengths and inlet temperatures were chosen in order to avoid sharp picks of temperature beyond 473 K (these combinations were probably not the optimal).

The strong effect of temperature on selectivity was particularly observed at the reactor entrance, showing that the reaction rate of the H_2 oxidation was clearly favored. This suggested that temperature should be lowered to enhance the selectivity towards CO oxidation.

It was also observed that, for a good exploitation of the O_2 (in the sense of selective CO oxidation), the last reactors had to be operated at an average lower temperature compared to the first ones: r_{CO} dropped significantly following the trend of CO partial pressure, whereas H_2 partial pressure remained essentially constant. Figs. 9 and 10a illustrate how O_2 was consumed at an increasing rate as CO was depleted, showing the

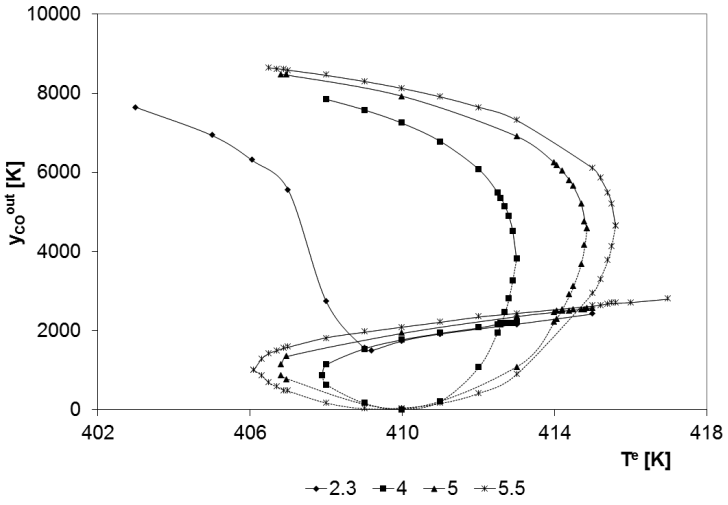

Figure 6. CO outlet molar fraction vs. RF inlet temperature for different *U* and countercurrent heat exchange.

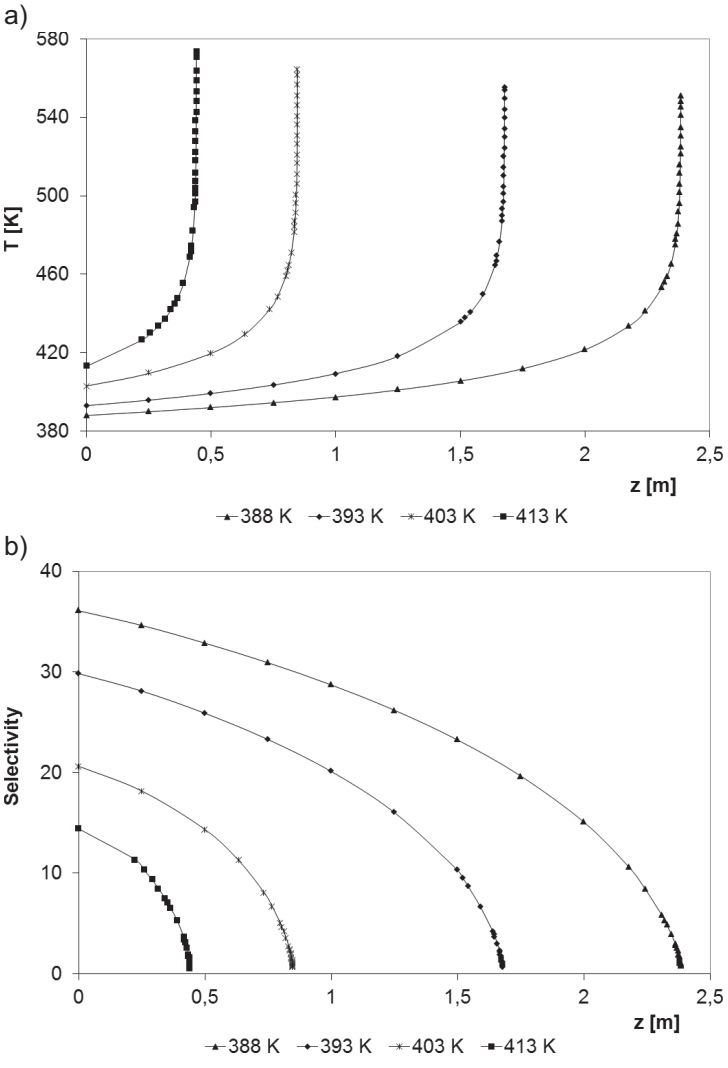

Figure 7. Profiles of temperature a) and selectivity b) for different T^e and fixed bed adiabatic operation.

importance of the H_2 oxidation reaction. Therefore, temperature had to be lowered to inhibit the H_2 oxidation. It is also shown in Figs. 9 and 10b that in the first half of the reaction volume, more than the 90 % of the CO was oxidized, and the second half, operated at lower temperature, left the stream in condition of entering the PEM fuel cell.

This scheme shows that six heat exchanges were sufficient to control the temperature rise. It was possible to achieve a CO concentration lower than 20 ppm with a H_2 conversion of around 2 % (nevertheless, attention should be paid to the H_2 conversion since both reaction extents were in the same order of magnitude). More precise reaction kinetics could show different results with respect to the number of reactors needed. However, it is important to note that the proposed scheme provides a means of temperature control.

As regards the heat exchange, distributing the RF in seven parts (the six heat exchanges plus an additional heat exchange to cool the outlet), the temperature requirements were be achieved. Considering a ΔT of approach larger than 25 K between the hot and cold streams, a rough calculation could help to choose the flow of HEF for each heat exchanged, according to

$$T^{c,out} = \frac{n_t \sum_j F_j \left[h_j\left(T_n^{out}\right) - h_j\left(T_{n+1}^{e}\right)\right]}{F_{T,n}^{c} \sum_j y_j^{c} Cp_j^{c}} + 298\text{K} \qquad (10)$$

4 Conclusions

A comparative study of different schemes of temperature control was performed. It was concluded from this work that temperature control was capital for the good performance of this stage. Two issues were highlighted: selectivity and water condensation.

The high exothermicity of both reactions involved in this process yielded a strong temperature increase which could be critical because of:

– catalyst sintering
– mechanical problems in the vessel
– loss of selectivity towards CO oxidation since the activation energy of this reaction is lower than that of H_2 oxidation

On the other hand, excessive heat removal causes an undesirable temperature drop which lowered the CO oxidation reaction and produced a stream out of specification. Moreover, water condensation would be a problem in this case.

The scheme that best kept temperature at the desired value was the series of adiabatic catalytic beds with interstage cooling. The reaction could be stopped, thus avoiding the runaway, choosing properly the bed lengths. This control was not possible with a single adiabatic reactor, which suffered from dramatic temperature increases and loss of selectivity. The series of adiabatic beds also allowed the energy integration: the water – ethanol reformer feed could be conveniently

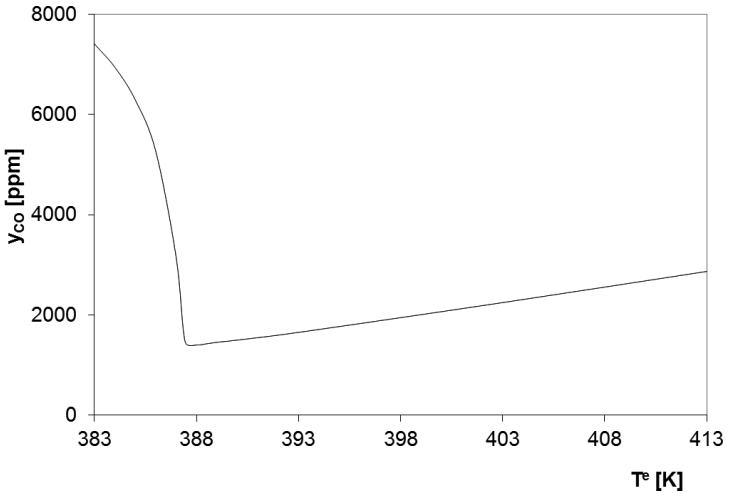

Figure 8. Effluent CO molar fraction vs. T^e for fixed bed adiabatic operation.

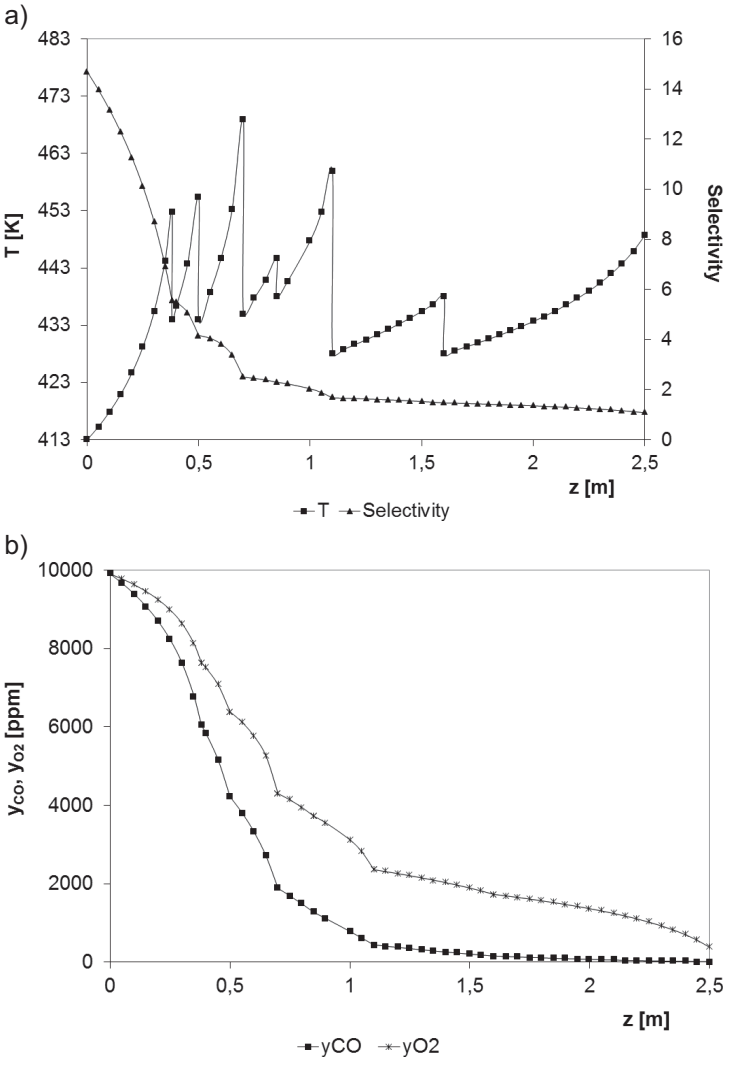

Figure 9. Profiles of a) temperature and selectivity, b) CO and O_2 mole fractions (T^e = 413 K) for a series of adiabatic fixed bed reactors with interstage cooling.

split in order to absorb heat from the RF while preheating itself.

The cocurrent operation was also a good alternative, but it had a strong sensitivity with respect to the value of U for CO conversions close to unity. The countercurrent operation was found to be unsuitable for the service required: for certain sets of values of U and T^e, multiplicity of steady states was present. Only the middle steady state was capable of reaching the 20 ppm. However, this steady state was unstable. For the other steady states, namely, the higher and lower ones, heat removal was either excessive or insufficient. The former led to temperature drop and condensation, and the latter to a runaway behavior. In both cases, the CO outlet was larger than 20 ppm. The alternative of employing a shorter reactor could solve the problem of temperature control, but still the CO fraction was found to be higher than 20 ppm. It was also concluded that the best way of increasing the selectivity was to overdimension the reactor and operate it at lower temperatures.

Acknowledgment

The authors gratefully acknowledge the financial support of ANPCYT, CONICET and the University of Buenos Aires.

The authors have declared no conflict of interest.

Symbols used

A_{CS}	[cm^2]	reactor cross-sectional area
c	[mol cm^{-3}]	concentration
C_p	[J $mol^{-1}K^{-1}$]	heat capacity
d_i	[cm]	reactor inside diameter
d_p	[cm]	inert solid diameter
E	[J mol^{-1}]	activation energy
F	[mol s^{-1}]	molar flow
G	[g s^{-1}]	total mass flow
g_c	[atm cm s^2g^{-1}]	unit change constant
h	[J mol^{-1}]	molar enthalpy
k	[mol $cm^{-3}s^{-1}atm^{-n}$]	kinetic coefficient
NC	[–]	number of species
NR	[–]	number of reactions
n_t	[–]	number of tubes
P	[atm]	total pressure
p	[atm]	partial pressure
r_i	[mol $cm^{-3}s^{-1}$]	reaction rate
S	[–]	selectivity
T	[K]	temperature
U	[J $cm^{-2}K^{-1}s^{-1}$]	overall heat transfer coefficient
x	[–]	conversion
y	[–]	mole fraction
z	[cm]	reactor axial variable

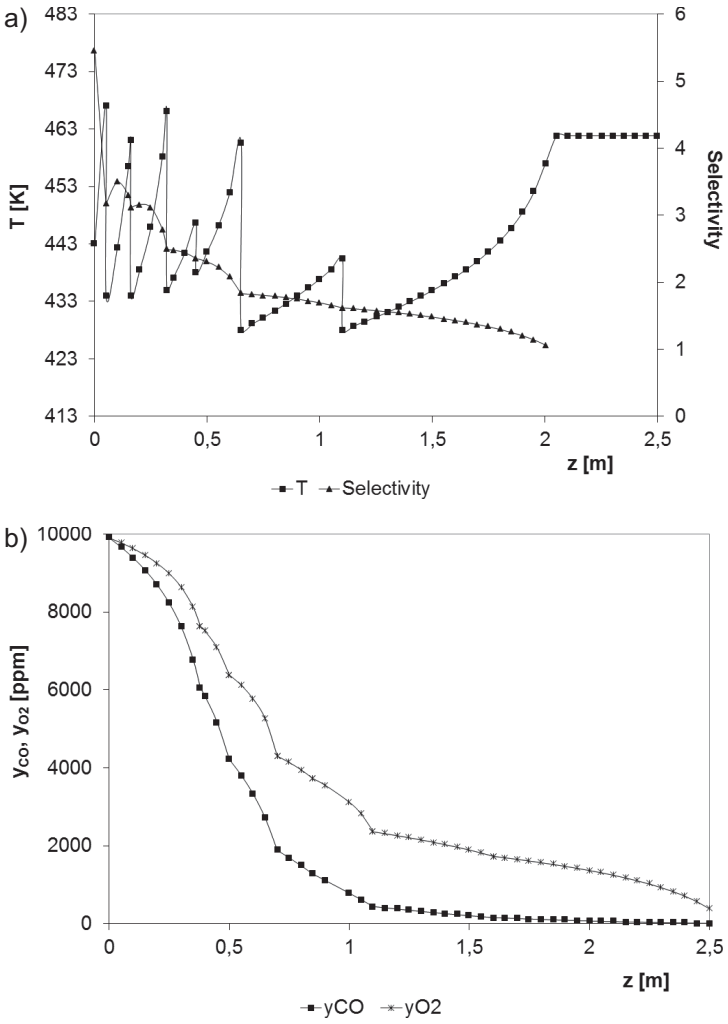

Figure 10. Profiles of a) temperature and selectivity, b) CO and O_2 mole fractions (T^e = 473 K) for a series of adiabatic fixed bed reactors with interstage cooling.

Greek letters

α	[–]	stoichiometric coefficient
ΔH_r	[J mol^{-1}]	reaction enthalpy
ε_B	[–]	catalytic bed porosity
η	[–]	effectiveness factor
μ	[Pa s]	viscosity of gas mixture
ρ	[g cm^{-3}]	density of gas mixture
ρ_B	[g cm^{-3}]	catalytic bed density

Subscripts and superscripts

c	heat exchanging fluid conditions
e	inlet conditions
out	outlet conditions
i	reaction *i*
j	species *j*
n	iteration step
sup	surface conditions
T	total

References

[1] P. Giunta, N. Amadeo, M. Laborde, *J. Power Sources* **2006**, *156*, 489. DOI: 10.1016/j.jpowsour.2005.04.036

[2] A. Sirijaruphan, J. Goodwin, R. Rice, *J. Catal.* **2004**, *227*, 547. DOI: 10.1016/j.jcat.2004.07.031

[3] J. Ayastuy, A. Gil-Rodriguez, M. Gonzalez-Marcos, M. Gutierrez-Ortiz, *Int. J. Hydrogen Energy* **2006**, *31*, 2231. DOI: 10.1016/j.ijhydene.2006.04.008

[4] E. Lopez, G. Kolios, G. Eigenberger, *Chem. Eng. Sci.* **2007**, *62*, 5598. DOI: 10.1016/j.ces.2006.12.087

[5] M. Echigo, N. Shinke, S. Takami, S. Higashiguchi, K. Hirai, T. Tabata, *Catal. Today* **2003**, *84*, 209. DOI: 10.1016/S0920-5861(03)00276-1

[6] F. Mariño, C. Descorme, D. Duprez, *Appl. Catal., B* **2005**, *274*, 285. DOI: 10.1016/j.apcatb.2004.12.008

[7] G. Sedmak, S. Hocevar, J. Levec, *J. Catal* **2003**, *213*, 135. DOI: 10.1016/S0021-9517(02)00019-2

[8] H. Lee, D. Kim, *Catal. Today* **2008**, *132*, 109. DOI: 10.1016/j.cattod.2007.12.028

[9] M. Moreno, G. Baronetti, M. Laborde, F. Mariño, *Int. J. Hydrogen Energy* **2008**, *33*, 3538. DOI: 10.1016/j.ijhydene.2008.03.043

[10] J. Zalc, D. Löfler, *J. Power Sources* **2002**, *111*, 58. DOI: 10.1016/S0378-7753(02)00269-0

[11] D. Oliva, J. Francesconi, M. Mussati, P. Aguirre, *J. Power Sources* **2008**, *182*, 307. DOI: 10.1016/j.jpowsour.2008.03.043

[12] S. Lee, J. Han, K. Lee, *J. Power Sources* **2002**, *109*, 394. DOI: 10.1016/S0378-7753(02)00096-4

[13] C. Dudfield, R. Chen, P. Adcock, *J. Power Sources* **2000**, *85*, 237. DOI: 10.1016/S0378-7753(99)00339-0

[14] C. Dudfield, R. Chen, P. Adcock, *Int. J. Hydrogen Energy* **2001**, *26*, 763. DOI: 10.1016/S0360-3199(00)00131-2

[15] F. Cipitì, V. Recupero, *Chem. Eng. J.* **2009**, *146*, 128. DOI: 10.1016/j.cej.2008.09.004

[16] F. Cipitì, L. Pino, A. Vita, M. Laganà, V. Recupero, *Int. J. Hydrogen Energy* **2007**, *32*, 4040. DOI: 10.1016/j.ijhydene.2007.04.046

[17] S. Zhou, Z. Yuan, S. Wang, *Int. J. Hydrogen Energy* **2006**, *31*, 924. DOI: 10.1016/j.ijhydene.2005.07.014

[18] V. Cominos, V. Hessel, C. Hoffmann, G. Kolb, R. Zapf, A. Ziogas, E. Delsman, J. Schouten, *Catal. Today* **2005**, *110*, 140. DOI: 10.1016/j.cattod.2005.09.008

[19] O. Goerke, P. Pfeifer, K. Schubert, *Appl. Catal., A.* **2004**, *263*, 11. DOI: 10.1016/j.apcata.2003.11.036

[20] X. Ouyang, L. Bednarova, R. Besser, P. Ho, *AIChE J.* **2005**, *51*, 1758. DOI: 10.1002/aic.10438

[21] M. O'Connell, G. Kolb, K. Schelhaas, J. Schuerer, D. Tiemann, A. Ziogas, V. Hessel, *Int. J. Hydrogen Energy* **2010**, *35*, 2317. DOI: 10.1016/j.ijhydene.2009.12.113

[22] L. Jeifetz, P. Giunta, M. Laborde, N. Amadeo, *17th CAC (Congreso Argentino de Catálisis)*, Salta, Argentina, October **2011**.

[23] B. Schönbrod, F. Mariño, G. Baronetti, M. Laborde, *Int. J. Hydrogen Energy* **2009**, *34*, 4021. DOI: 10.1016/j.ijhydene.2009.02.054

[24] W. Liu, M. Flytzani-Stephanopolous, *J. Catal.* **1995**, *153*, 317. DOI: 10.1006/jcat.1995.1133
[25] M. Moreno, L. Bergamini, G. Baronetti, M. Laborde, F. Mariño, *Int. J. Hydrogen Energy* **2010**, *35*, 5918. DOI: 10.1016/j.ijhydene.2009.12.107
[26] P. Giunta, C. Mosquera, N. Amadeo, M. Laborde, *J. Power Sources* **2007**, *164*, 336. DOI: 10.1016/j.jpowsour.2006.09.091
[27] P. Giunta, N. Amadeo, M. Laborde, *Int. J. Chem. Reactor Eng.* **2008**, *6*, A12.
[28] P. Giunta, N. Amadeo, M. Laborde, L. Bergamini, *AIChE J.* **2011**, *57*, 473. DOI: 10.1002/aic.12267.
[29] B. Finlayson, *Nonlinear Analysis for Chemical Engineering*, McGraw-Hill, New York **1980**.

Research Article: Preferential oxidation of CO with a Cu/CeO_2 catalyst was employed to reduce the CO content to less than 20 ppm in a hydrogen stream obtained from hydrocarbons or alcohols. Temperature control is a key issue to achieve high CO conversion and simultaneously to avoid the oxidation of hydrogen. Heat transfer alternatives in a fixed bed reactor are analyzed and discussed.

COPROX Fixed Bed Reactor – Temperature Control Schemes

P. Giunta, M. Moreno, F. Mariño*, N. Amadeo, M. Lobarde

Chem. Eng. Technol. **2012**, *35* (■), XXX ... XXX

DOI: 10.1002/ceat.201100644